$$W_\alpha = \frac{S_\alpha (ZMV)_\alpha}{\sum_{k=1}^{n} S_k (ZMV)_k}. \qquad (3.9.26)$$

The use of equation (3.9.26) in QPA again eliminates the need to measure the instrument calibration constant and estimate the sample mass absorption coefficient. However, the necessity of normalizing the sum of the analysed weight fractions to unity only produces the correct *relative phase abundances*. This approach is the most widely used in Rietveld-based QPA and is almost universally coded into Rietveld analysis programs. If the sample contains amorphous phases and/or minor amounts of unidentified crystalline phases, the analysed weight fractions will be overestimated. Where absolute phase abundances are required in, for example, the derivation of reaction mechanisms in *in situ* studies, then one of the methods that produces absolute phase abundances must be used.

3.9.4. Demonstration of methods

The sample 1 suite from the IUCr Commission on Powder Diffraction (CPD) round robin on QPA (Madsen *et al.*, 2001) provides a useful basis for demonstrating the applicability some of the methods described above. Sample 1 was designed to provide a relatively simple analytical system in order to determine the levels of accuracy and precision that could be expected under ideal conditions. The key design criteria required that the phases exhibit little peak overlap in the low-angle region of the diffraction pattern and the samples have at least one freestanding peak for each phase in the *d*-spacing range 3.7 to 1.9 Å.

The three components (corundum, α-Al_2O_3; fluorite, CaF_2; and zincite, ZnO) were prepared in a ternary design to provide a total of eight different mixtures in order to cover as wide a range of composition as possible for each phase. The result is that each phase is present in the suite with concentrations of approximately 1, 4, 15, 33, 55 and 95 wt%. The exact compositions (Madsen *et al.*, 2001) can be found in Table 3.9.1. The unique chemical composition of the component phases also allowed the weighed compositions to be confirmed by measurement of total elemental composition using X-ray fluorescence (XRF) methods.

Data sets were collected from three replicates of the eight mixtures using a Philips X'Pert diffractometer equipped with a Cu long fine focus tube operated at 40 kV and 40 mA. The beam path was defined with 1° divergence, 0.3 mm receiving and 1° scatter slits. A curved graphite post-diffraction monochromator was fitted to eliminate $K\beta$ radiation. Data were collected from 15 to 145° 2θ in increments of 0.02° using a counting time of 1.5 s per step. These data sets are available as supporting information from http://it.iucr.org/ for any reader wishing to develop and test their skills in various methods.

For the single-peak methods, the net intensity for all peaks in the range 22 to 65° 2θ was extracted using a fundamental-parameters approach to peak fitting coded in the *TOPAS* software package (Bruker AXS, 2013). The choice of peak profile type is important, since any misfit will be reflected in the estimation of peak area and hence in the QPA. Unless otherwise stated, QPA was undertaken using the strongest peak in the pattern for each phase (corundum 113, d = 2.085 Å; fluorite 022, d = 1.932 Å; zincite 011, d = 2.476 Å). The average values for these peaks can be found in Table 3.9.2. For those methods requiring knowledge of the mass absorption coefficient, μ_m^* for each sample was calculated from the XRF chemical analysis results.

Table 3.9.1
Weighed composition (weight fraction) of the eight mixtures comprising sample 1 in the IUCr CPD round robin on QPA (Madsen *et al.*, 2001)

Sample	Corundum	Fluorite	Zincite
1A	0.0115	0.9481	0.0404
1B	0.9431	0.0433	0.0136
1C	0.0504	0.0136	0.9359
1D	0.1353	0.5358	0.3289
1E	0.5512	0.2962	0.1525
1F	0.2706	0.1772	0.5522
1G	0.3137	0.3442	0.3421
1H	0.3512	0.3469	0.3019

Table 3.9.2
Average values (n = 3) of net peak intensity derived using profile fitting for the strongest peaks of corundum (113), fluorite (022) and zincite (011)

The figures in parentheses are the standard deviations of the means. The sample mass absorption coefficient μ_m^* was calculated from the XRF-L determined composition.

Sample	Corundum	Fluorite	Zincite	μ_m^* (cm^2 g^{-1})
1A	34.8 (0.6)	8958.7 (33.0)	509.9 (6.0)	93.02
1B	6561.3 (28.6)	1095.5 (7.1)	474.3 (3.8)	34.45
1C	244.4 (0.9)	250.9 (10.1)	22898.0 (37.0)	49.03
1D	474.5 (3.5)	6559.6 (2.8)	5468.5 (9.5)	71.71
1E	2525.3 (27.9)	4835.5 (27.0)	3370.7 (16.3)	53.17
1F	1251.3 (7.8)	2935.8 (9.0)	12494.9 (22.4)	52.67
1G	1295.0 (8.7)	5041.7 (17.0)	6787.9 (26.6)	59.64
1H	1436.5 (7.3)	5132.0 (13.6)	5996.8 (59.5)	59.10

3.9.4.1. *Absorption–diffraction method*

In this method, the QPA of each phase is conducted independently of the others. For each phase, the determination of a specific calibration constant, C, was achieved using a rearranged equation (3.9.3). The sample where the relevant phase was present at about 55 wt% (sample 1E for corundum, 1D for fluorite and 1F for zincite) was taken to be the calibration sample.

For fluorite the determination of C proceeded using

$$C_{i,\alpha} = I_{i,\alpha} \frac{\mu_m^*}{W_\alpha} = 6559.6 \times \frac{71.71}{0.5358} = 877\,919. \qquad (3.9.27)$$

All data sets were then analysed using equation (3.9.3), as demonstrated here using sample 1H.

$$W_\alpha = I_{i,\alpha} \frac{\mu_m^*}{C_{i,\alpha}} = 5132.0 \times \frac{59.1}{877919} = 0.3455, \qquad (3.9.28)$$

compared with a value of 0.3469 added to the sample by weight. Fig. 3.9.1 shows the analysed concentration for all 24 fluorite measurements along with the bias from the known values. The bias (analysed − known) all fall within the range −0.3 to 0.5 wt% with no systematic bias as a function of concentration. The similar results achieved for corundum and zincite demonstrate the validity of the approach where there is minimal peak overlap.

3.9.4.2. *Internal standard method*

Application of the internal standard method normally requires the addition of an appropriate phase in known amount to each sample to be analysed. In order to use this data for demonstration of the internal standard method, it is necessary to designate one of the existing phases as the internal standard. Sample 1H has been used to derive the calibration constant, with fluorite considered to be the phase of interest while zincite is designated

as the internal standard. The intensities (Table 3.9.2) and known concentrations (Table 3.9.1) of these phases can then be used to derive $C_{\alpha s}^{ij}$ from equation (3.9.8) to eliminate the need to know or measure μ_m^* for the sample.

$$\frac{I_{\text{fluorite}}}{I_{\text{zincite}}}\frac{W_{\text{zincite}}}{W_{\text{fluorite}}} = C_{\alpha s}^{ij} = \frac{5132.0}{5996.8} \times \frac{0.3019}{0.3469} = 0.7448. \qquad (3.9.29)$$

Analysis of the unknowns (Fig. 3.9.2) then proceeds *via* equation (3.9.9) and is demonstrated here using sample 1D:

$$W_{\text{fluorite}} = \frac{W_{\text{zincite}}}{C_{\alpha s}^{ij}}\frac{I_{\text{fluorite}}}{I_{\text{zincite}}} = \frac{0.3289}{0.7448}\frac{6559.6}{5468.5} = 0.5297, \qquad (3.9.30)$$

compared with a value of 0.5358 added to the sample by weight.

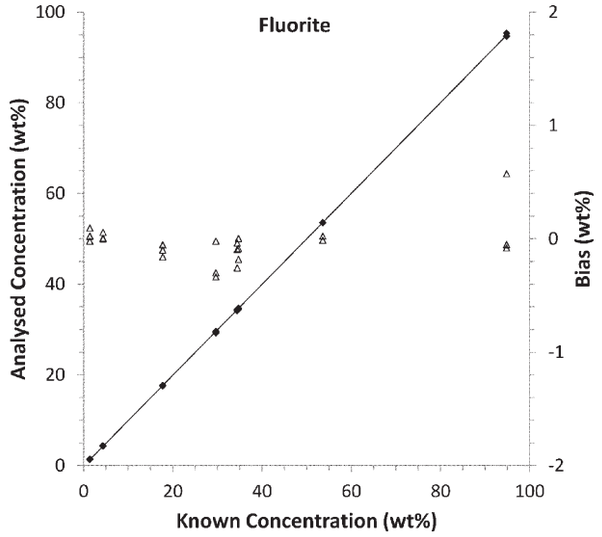

Figure 3.9.1
Plot of the analysed concentration (black diamonds – left axis) and the bias (open triangles – right axis) expressed as wt% for fluorite using the absorption–diffraction method. The analysis was calibrated using sample 1D, which has a fluorite concentration of 53.58 wt%.

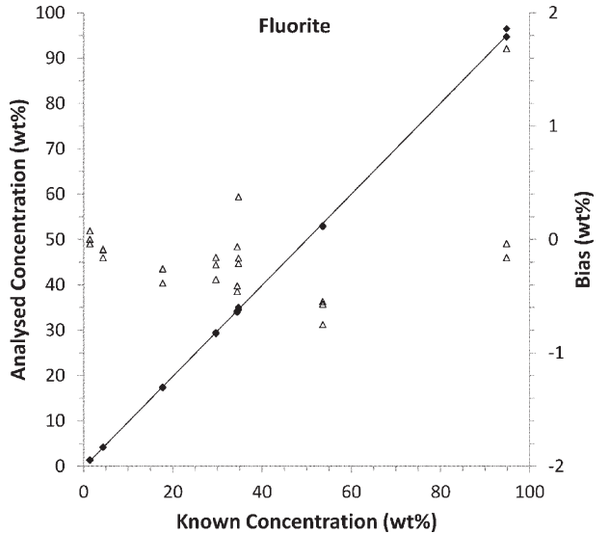

Figure 3.9.2
Plot of the analysed concentration (black diamonds – left axis) and the bias (open triangles – right axis) expressed as wt% for fluorite using the internal standard method with zincite designated as the internal standard. The analysis was calibrated using sample 1H where the fluorite and zincite concentrations are 34.69 and 30.19 wt%, respectively.

3.9.4.3. *Reference intensity ratio*

For this exercise, the peak intensities and phase concentrations in Tables 3.9.1 and 3.9.2 for sample 1H can be used to determine the RIRs for fluorite and zincite.

$$\text{RIR}_{\text{fluorite}} = \frac{5132.0}{1436.5} \times \frac{0.3512}{0.3469} = 3.617, \qquad (3.9.31)$$

$$\text{RIR}_{\text{zincite}} = \frac{5996.8}{1436.5} \times \frac{0.3512}{0.3019} = 4.856. \qquad (3.9.32)$$

These RIRs should be compared with reported values for fluorite in the ICDD database (ICDD, 2015) which have an average of 3.83 (n = 33) but range from 2.40 to 4.21. For zincite the reported RIR values have an average of 5.24 (n = 50) and range from 4.50 to 5.87. The discrepancies in the various reported values of the RIRs highlight the need to determine them under the same conditions as the samples being analysed if the highest accuracy is to be achieved.

Fig. 3.9.3 shows the RIR values calculated from all 24 (eight samples, three replicates each) measurements for fluorite and zincite plotted as a function of corundum concentration. At intermediate concentrations there is quite good agreement between the determined values. However, there are significant deviations at low corundum concentration, resulting in insufficient measured intensity in the corundum peak to ensure sufficient accuracy in the RIR. Hence, care should be taken to ensure that there are sufficient counts in the peaks used to determine the RIR. In addition, a low concentration automatically means that there are fewer grains contributing to the diffraction process; hence particle statistics may also present a significant problem.

The presence of other sample-related aberrations that affect the measured intensities also needs to be considered. For example, microabsorption may affect measured RIR values differently in different concentration ranges. The impact of such effects on the analysis is reduced by their inclusion in the measured RIR provided that variation induced by, for example, sample preparation can be kept to a minimum.

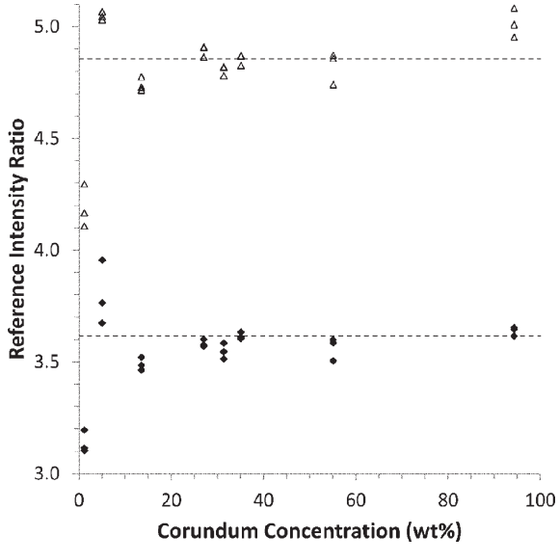

Figure 3.9.3
Plot of the 24 determined RIR values for fluorite (black diamonds) and zincite (open triangles) as a function of corundum concentration. The dashed lines represent the average RIR values for fluorite (lower) and zincite (upper) determined from the three replicates of sample 1H where all phases have approximately equal concentration.

references